Counting anti-protons with an MCP-SiPM setup to determine the absolute number of anti-protons in the ALPHA experiment

Stine Svanum Frederiksen
Supervisor: Steven Armstrong Jones

August 18, 2022

1 Introduction

The ALPHA collaboration traps and studies anti-hydrogen ($\bar{\mathrm{H}}$) in order to search for subtle differences between matter and anti-matter. The goal of this project has been to improve the experimental techniques to compare hydrogen (H) to $\bar{\mathrm{H}}$.

So far, $\bar{\mathrm{H}}$ spectroscopy has relied on causing the atoms to annihilate, and detecting those annihilations. These annihilations are detected by the ALPHA-II silicon vertex detector (SVD). The efficiency of this detector is well known, however, this detection method is not compatible with H atoms, as they will not cause annihilation events with the material of the trap walls.

This project has therefore focused on developing an alternative detection method where the H or $\bar{\mathrm{H}}$ is first ionised, and the proton (p) or anti-proton ($\bar{\mathrm{p}}$) can be detected using a multichannel plate detector (MCP) and silicon photo multiplier (SiPM). As this allows detection of H and $\bar{\mathrm{H}}$s in the same trap, it thus aims to improve on the systematic errors related to measuring the two species separately. This is especially applicable in ALPHA's spectroscopy setup, where the species are ionized by lasers.

We first wish to determine the absolute efficiency of the SiPM to know how many $\bar{\mathrm{p}}$s are in a trap based on the results of our measurements. With this, the absolute number of $\bar{\mathrm{p}}$s can be determined in various parts of the experiment.

2 Counting setup & Methods

2.1 Micro-channel plate / phosphor screen & SiPM

The micro-channel plate (MCP) / phosphor screen detector is a device which is found at several positions in the experimental setup. Its function is to detect charged particles and emit light to be imaged on a camera or detected on a SiPM.

The voltages on the front and back of the MCP as well as on the phosphor screen are all adjustable. The voltage on the front plate accelerates charged particles towards the detector and can therefore control the impact energy of the particles on the detector. The charged particles will initiate cascades of electrons in the channels of the MCP, and the voltage on the back plate relative to the front controls the gain [1]. Finally, the voltage on the phosphor screen is kept higher than that of the back plate, so the amplified charge hits the phosphor and light is emitted to be collected by a camera or SiPM (see Fig. 2 for illustration). The phosphor screen is kept at 5 kV in order to produce light which can be picked up by the SiPM.

There are several MCP-SiPM setups in the ALPHA experiment. An overview of the relevant parts for this project is shown in Fig. 1. The CT (catching trap) stick can image the $\bar{\mathrm{p}}$s arriving from the catching trap — the place where they are initially caught when arriving from the anti-proton decelerator (AD) and ELENA (The Extra Low Energy Antiproton ring). Similarly, there is an AT stick that can image the $\bar{\mathrm{p}}$s from the ALPHA-II atom trap (AT). The LDS (lower

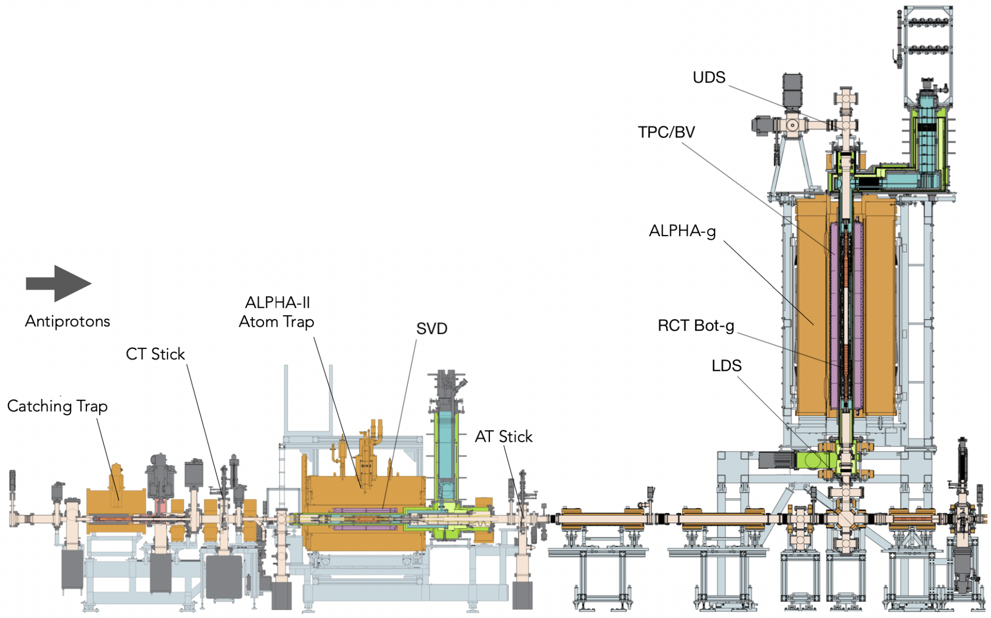

Figure 1: Schematic of part of the ALPHA experiment. Modified from [2].

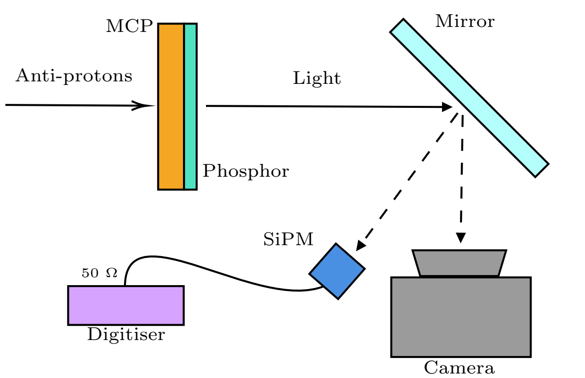

Figure 2: Illustration of the setup of the MCP-SiPM and camera. $\bar{\text{p}}$s are accelerated onto the MCP, and a cascade of electrons is produced, which hits the phosphor screen from which light is emitted and sent towards a mirror. The light is reflected to reach a camera and a SiPM.

diagnostics station) sits at the bottom of ALPHA-g and has two MCPs: the "upstream" (US) MCP, which faces towards the incoming $\bar{\text{p}}$s from the CT, and a "downstream" (DS) MCP, which faces in the opposite direction towards the ALPHA-g traps. The MCP we are using is the Photonis APD 1 PS 40/12/10/12 I 60:1 EDR P46.

2.2 Pulse analysis

In order to calibrate the MCP-SiPM setup, it was necessary to be able to count individual $\bar{\text{p}}$s arriving at the detector. A peak-finding program was developed in LabView, but in order to resolve the individual particles, it was also necessary to change settings of the experiment to slowly dump (approximately) one $\bar{\text{p}}$ at a time onto the MCP to avoid saturation. During such a dump of particles, the walls of the potential trapping the plasma are lowered in the direction of the detector, so the particles spill out of the trap and onto the detector.

Previously, a plasma of $\bar{\text{p}}$s was dumped to the MCP

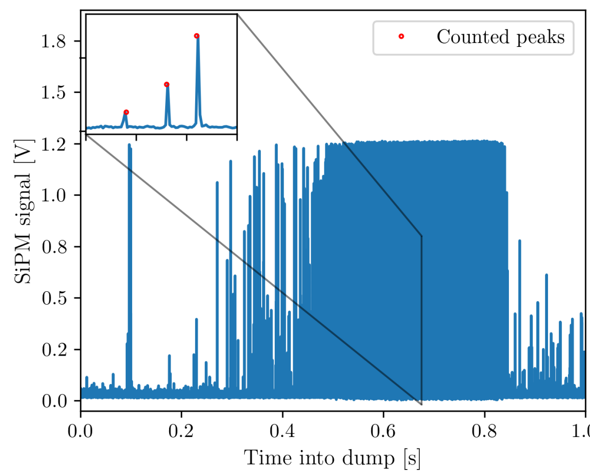

Figure 3: SiPM signal at CT MCP for 1000 V gain and 50 Ω termination directly to digitiser. The zoom window shows that we can resolve individual peaks using this method. To keep the plot simple, the counted peaks are only plotted in the zoom window.

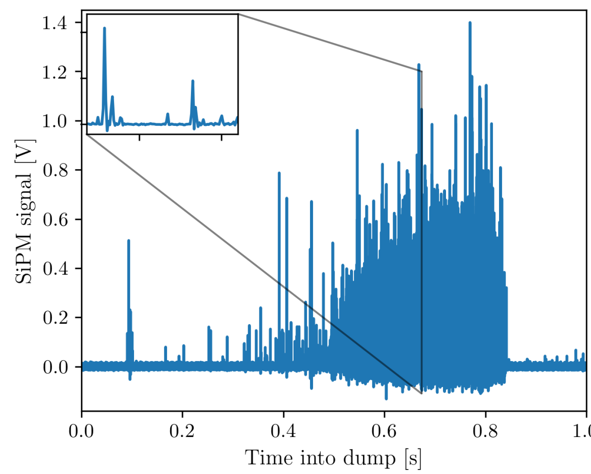

Figure 4: SiPM signal when SiPM is connected to preamplifier with a gain of 1 and MCP gain of 1000 V. Ringing of the signal is apparent.

as fast as possible so they all arrived somewhat simultaneously. The new dump time was adjusted to be 1 s in total. This included a pre-dump of 100 ms to eject the fastest particles, a slow dump at 800 ms for the majority of the particles, and finally 100 ms post-dump to eject particles far off-axis. An example signal is shown on Fig. 3.

The SiPM was originally connected to a pre-amplifier, and we investigated its slow and fast outputs for different gains of 1, 10, and 100. We found no reason for upping the gain, so we kept it at 1 on the slow output of the SiPM. Having the SiPM connected to the pre-amplifier, however, proved to cause ringing in the cables (see Fig. 4) which made peak diagnostics more difficult. For this reason, we connected the output directly to a digitiser/scope with a 50 Ω termination.

The digitiser used for most of the diagnostics sticks is the PCI-6132 from National Instruments, which can sample at a rate of 2.5 MS per second. It was investigated whether this digitiser is actually fast enough to count all the $\bar{\text{p}}$s arriving at the MCP. For this purpose, the slow output of the SiPM was connected to a 10 MS per second scope (Wavesurfer 3034) and the signal was compared to that obtained with the PCI-6132.

One thing we observed with the faster scope is the presence of zone noise (high frequency wavepackets picked up from the accelerator operations). The advantage of the slower scope is that this noise is averaged over and does therefore not add to the background counts. A disadvantage of the slower scope is that it seems to occasionally combine two distinct peak into one, because it cannot resolve them. On the other hand, the fast scope seems to double or even triple count some peaks, causing an overestimation of counts. In the end, the big drawback of the fast scope for this analysis was data extraction — the scope will only write to a flash drive smaller than 512 MB, and the files we saved were of size ∼200 MB, so we stuck with the PCI-6132.

To determine when to count a peak as a $\bar{\text{p}}$, different cut-off thresholds for the peak amplitudes were applied to the background measurements and the measurements with $\bar{\text{p}}$s. Measurements on the CT stick are shown in Fig. 5.

Determining the cut-off threshold to optimize the signal-to-noise ratio is not a straight-forward issue to solve. As seen in Fig. 6, the background counts at the

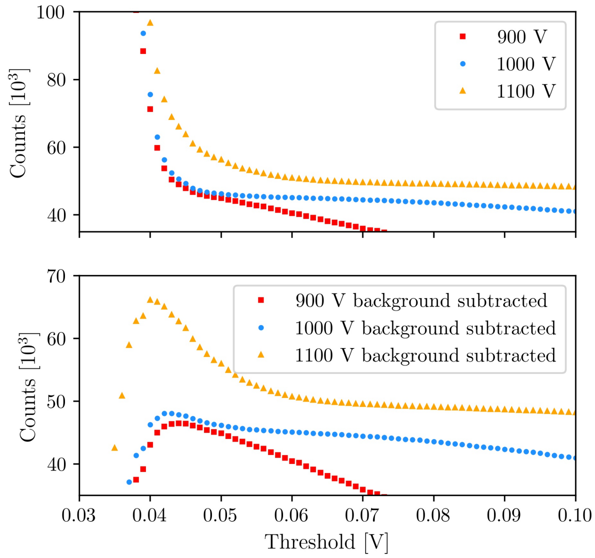

Figure 5: Threshold scans of the CT SiPM signal with (top) and without (bottom) subtracted background.

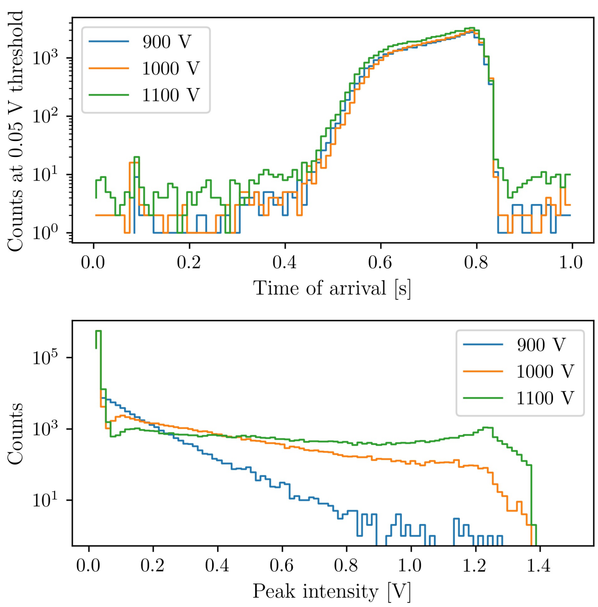

Figure 6: Time (top) and intensity (bottom) distributions of counts at the CT stick for different MCP gains. The SiPM saturates at ~1.3 V, causing the sharp drop in counts for high intensity in the lower plot.

CT MCP are particularly hard to distinguish from the actual signal for an MCP gain of 900 V. We see the count number for the 1100 V gain start to stabilise at a threshold of around 0.06 V. The background counts at this threshold and gain are of the order of 100 counts. Because the gain of 1100 V is least sensitive to the threshold, this setting is kept for the CT MCP. The approach for the other MCPs is much the same, with exception of the LDS DS MCP, for which we had no background measurements. Hence, the threshold scan was examined carefully to determine when most of the background had been cut off. A summary of the optimal settings found for this and the other MCPs in the experiment can be found in Table 1.

MCP	Gain [V]	Threshold [V]
CT	1100	0.06
AT	1100	0.02
LDS US	1000	0.0105
LDS DS	1000	0.012

Table 1: Current optimal settings for the various MCPs in the experiment.

To determine the efficiency of this counting method, we cross-calibrated with the AT SVD. We catch the $\bar{p}$s and cause them to be lost radially within the detector volume. The SVD can detect the annihilations of the $\bar{p}$s with the trap wall with a trigger efficiency of 88 % [3]. From 8 successful runs, we then see that we are catching $53\,000 \pm 400$ $\bar{p}$s in the AT. The efficiency of the new counting method is then found by catching $\bar{p}$s in the AT and imaging them on the AT MCP and comparing the counts obtained with that of the SVD. Results are presented in the following section.

3 Results

With an MCP gain of 1100 V and peak detection threshold of 0.06 V, the measurement from the AT to the AT MCP gave a count of $49\,000 \pm 2\,000$. Comparing with the SVD counts, this suggests an efficiency of 93 ± 4 % of the MCP-SiPM detection method for $\bar{p}$s.

With the settings from Table 1 and applying the efficiency to the results, we find estimates for the number of $\bar{p}$s at different points in the experiment — these are shown in Table 2. Additionally, some background measurements at the same settings are collected in Table 3.

From	To MCP	Calibrated $\bar{p}$ counts
CT	CT	$55\,000 \pm 2\,000$
CT	AT	$54\,000 \pm 2\,000$
AT	AT	$53\,000 \pm 3\,000$
CT	LDS US	$55\,000 \pm 2\,000$
RCT Bot-g	LDS DS	$25\,000 \pm 1\,000$

Table 2: Number of $\bar{p}$s detected by the MCP-SiPM setup from and to various places in the experiment. The efficiency of $93 \pm 4\,\%$ has been applied to all counts, assuming that the efficiency is the same of all the MCP-SiPM setups. Uncertainties are given by the variances of different runs. Note that there was only one run done at the settings in Table 1 for the CT MCP and the uncertainty is therefore based only on the uncertainty on the efficiency.

The results suggest that the transfers from the catching trap all the way up to the LDS are very efficient, as the $\bar{p}$ counts for these MCP-SiPM setups are within error of each other. On the other hand, we see that when the $\bar{p}$s are re-captured in ALPHA-g and imaged afterwards on the LDS, there is significant loss — only about 47 % of the $\bar{p}$s are left.

MCP	Background counts
CT	130 ± 20
AT	124 ± 6
LDS US	110 ± 6

Table 3: Background counts detected by the MCP-SiPM setup from and to various places in the experiment.

4 Discussion & Conclusion

The $\bar{p}$ counting method developed proves to detect nearly all $\bar{p}$s that hit the MCP — at an efficiency of $93 \pm 4\,\%$, this is a handy setup to detect individual $\bar{p}$s, with the advantage that there are many MCPs at different positions in the experiment — more than what we have investigated in this project.

The $\bar{p}$ detection efficiency of our MCP is higher than its known detection efficiency of protons, which lies at ∼55 % (this can be improved to ∼86 % with a funnel MCP) [4]. The proton detection efficiency is highly limited by the geometry of the standard MCP, where there is dead-space between the circular-shaped channels. For $\bar{p}$s, we suspect that the geometry matters less due to the annihilation products (of which there are typically 2-3 charged pions [5]) of the $\bar{p}$s on the MCP channels, which can trigger channels even though the $\bar{p}$ hits a dead-spot on the MCP. The result of $93 \pm 4\,\%$ obtained for the $\bar{p}$ detection efficiency of our MCP supports this idea.

Following the calibration of the setup, the number of $\bar{p}$s was determined at several points in the ALPHA experiment. Of particular interest is the number of $\bar{p}$s in ALPHA-g, which suggests a loss of about 53 % when the $\bar{p}$s are re-captured in the bottom trap of ALPHA-g. Similarly, there is an MCP at the top of ALPHA-g not used in this project, which would be obvious to investigate in the future to validate this even further.

In ALPHA-g, the annihilation of the $\bar{H}$s is detected with the radial time projection chamber / barrel veto (TPC/BV). This detection method has not yet been calibrated to give an absolute number of $\bar{H}$s, but studies of the LDS and UDS MCPs with the methods outlined in this project pave the way for a future cross-calibration.

In general this investigation will benefit from more statistics in the future. The measurement at the optimal settings for the CT MCP in particular was only done once and hence should be repeated.

For the purpose of this project — finding the number of $\bar{p}$s at different MCPs — the background counts observed at the chosen threshold were on the order of 100. This is acceptable because we have been measuring 20 000+ $\bar{p}$s, but if the setup should be used to detect for example less than 10 $\bar{p}$s, such as could be the case when $\bar{H}$s have been trapped and ionised, the background should be analysed more carefully to keep it $\ll$10. For this case, a higher threshold is desired, as it more clearly separates the $\bar{p}$ counts from the background. Additionally, one could consider a shorter dump time to reduce the background counts, since there are much less $\bar{\text{p}}$s to dump than the case studied in this project.

References

[1] G. B. Andresen et al., “Antiproton, positron, and electron imaging with a microchannel plate/phosphor detector”, Review of Scientific Instruments **80**, 123701 (2009) 10.1063/1.3266967.

[2] M. A. Johnson, “Design and commissioning of beamlines for the alpha antihydrogen experiment”, PhD thesis (The University of Manchester, 2019).

[3] C. Amole et al., “The alpha antihydrogen trapping apparatus”, Nuclear Instruments and Methods in Physics Research Section A: Accelerators, Spectrometers, Detectors and Associated Equipment **735**, 319–340 (2014) 10.1016/j.nima.2013.09.043.

[4] K. Fehre et al., “Absolute ion detection efficiencies of microchannel plates and funnel microchannel plates for multi-coincidence detection”, Review of Scientific Instruments **89**, 045112 (2018) 10.1063/1.5022564.

[5] W. A. Bertsche et al., “Physics with antihydrogen”, Journal of Physics B: Atomic, Molecular and Optical Physics **48**, 232001 (2015) 10.1088/0953-4075/48/23/232001.